

# Poly(trehalose): Sugar-Coated Nanocomplexes Promote Stabilization and Effective Polyplex-Mediated siRNA Delivery

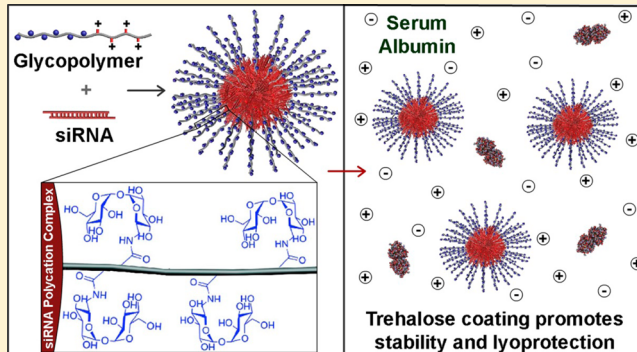
Antons Sizovs,<sup>†,§</sup> Lian Xue,<sup>‡</sup> Zachary P. Tolstyka,<sup>‡</sup> Nilesh P. Ingle,<sup>‡</sup> Yaoying Wu,<sup>‡</sup> Mallory Cortez,<sup>‡</sup> and Theresa M. Reineke\*,<sup>†,‡</sup>

<sup>†</sup>Department of Chemistry and Macromolecules and Interfaces Institute, Virginia Tech, Blacksburg, Virginia 24060, United States

<sup>‡</sup>Department of Chemistry, University of Minnesota, 207 Pleasant Street SE, Minneapolis, Minnesota 55455, United States

## Supporting Information

**ABSTRACT:** When nanoparticles interact with their environment, the nature of that interaction is governed largely by the properties of its outermost surface layer. Here, we exploit the exceptional properties of a common disaccharide, trehalose, which is well-known for its unique biological stabilization effects. To this end, we have developed a synthetic procedure that readily affords a polymer of this disaccharide, poly(methacrylamidotrehalose) or “poly(trehalose)” and diblock copolymerizations containing this polymer with 51 repeat units chain extended with aminoethylmethacrylamide (AEMA) at three degrees of polymerization ( $n = 34, 65$ , and  $84$ ). Two series of experiments were conducted to study these diblock copolymers in detail and to compare their properties to two control polymers [PEG-P(AEMA) and P(AEMA)]. First, we demonstrate that the poly(trehalose) coating ensures colloidal stability of polyplexes containing siRNA in the presence of high salt concentrations and serum proteins. Poly(trehalose) retains the ability of trehalose to lower the phase transition energy associated with water freezing and can protect siRNA polyplexes during freeze-drying, allowing complete nanoparticle resuspension without loss of biological function. Second, we show that siRNA polyplexes coated with poly(trehalose) have exceptional cellular internalization into glioblastoma cells that proceeds with zero-order kinetics. Moreover, the amount of siRNA delivered by poly(trehalose) block copolymerizations can be controlled by the siRNA concentration in cell culture media. Using confocal microscopy we show that trehalose-coated polyplexes undergo active trafficking in cytoplasm upon internalization and significant siRNA-induced target gene down-regulation was achieved with an  $IC_{50}$  of  $19\text{ nM}$ . These findings coupled with a negligible cytotoxicity suggests that poly(trehalose) has the potential to serve as an important component of therapeutic nanoparticle formulations of nucleic acids and has great promise to be extended as a new coating for other nanobased technologies and macromolecules, in particular, those related to nanomedicine applications.



## INTRODUCTION

Materials that promote the stabilization of macromolecules and nanosystems from nonspecific interactions and colloidal aggregation, while still retaining function on the nanoscale, are of high general interest to many fields. For over 40 years, poly(ethylene glycol) (PEG) has served as the gold standard for surface coating due to its solubility in both organic and aqueous media, large hydration volume, conformational flexibility, and general low level of immunogenicity and toxicity, supporting its use in medical applications.<sup>1</sup> Various nanomedicine carrier systems are routinely stabilized with PEG to prevent aggregation, nonspecific interactions, and premature in vivo clearance, promoting “stealth”-like properties.<sup>1</sup> For these reasons, PEG is the primary polymer for use in current drug, protein, and nucleic acid bioconjugates that have been FDA approved. However, the ubiquitous use of PEG in personal care and pharmaceutical products has shed new light on possible drawbacks of this material.<sup>1</sup> For example, adverse events have been found in some cases of PEGylated nanosystems such as

hypersensitivity reactions<sup>2,3</sup> antibody generation,<sup>4</sup> and accelerated blood clearance.<sup>5–7</sup> In addition, questions with regard to the long-term oxidative stability<sup>8,9</sup> and thermal stability<sup>10</sup> of PEG and challenges in the patent landscape have contributed to heightened interest in new stealth materials for macromolecules and nanosystems.<sup>1</sup>

Nature offers creative and sustainable alternatives to promote nanosystem stabilization, through the use of carbohydrates. Indeed, the disaccharide,  $\alpha$ - $\alpha$ -D-trehalose, is endowed with special properties ideal for use in stealth materials research and development. This nonreducing disaccharide is composed of two  $\alpha$ -1-linked glucose units and is very stable to acidic hydrolysis, even at high temperatures.<sup>11</sup> Trehalose is biosynthesized in many organisms but not in humans; however, the enzyme trehalase is expressed in humans, which promotes metabolism into glucose. Trehalose has been found in many

Received: May 16, 2013

Published: October 1, 2013

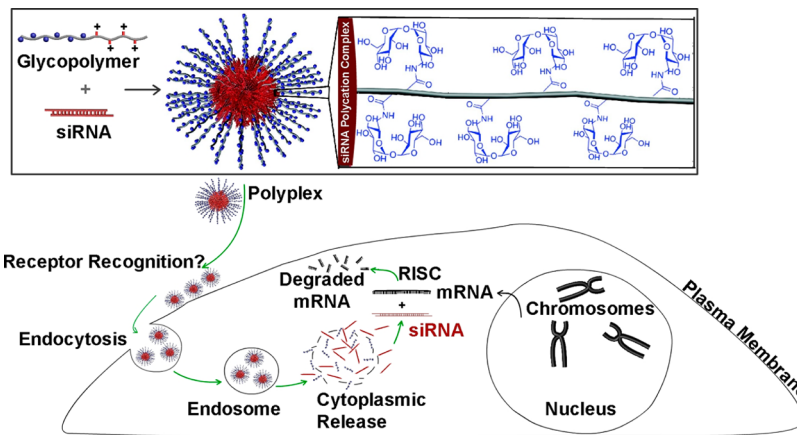


**Figure 1.** Schematic of polyplex formation with siRNA and poly(trehalose) block copolyacrylates, cellular internalization, and gene knockdown.

organisms and protects cells during oxidative stress<sup>12</sup> and freezing<sup>13,14</sup> and is known to aid in cryptobiosis. Trehalose is also found and accumulated under stress in a number of plants, animals, and insects with cryptobiotic ability (e.g., tardigrades<sup>15,16</sup>). For example, exposure of a desiccated resurrection plant, *Selaginella lepidophylla*, to water leads to a remarkable restoration of normal metabolism that occurs within hours; about 90% of the total plant sugar in this species is trehalose.<sup>17</sup>

The opportunities for exploiting these properties for materials research and nanoparticle stabilization have just begun. Trehalose has enabled freezing, freeze-drying, and hypothermal storage of various macromolecules including proteins, antibodies, DNA, liposomes, DNA/lipid complexes, cells and even organs.<sup>18</sup> We have shown that step-growth cationic polymers containing alternating units of ethylene-amines and trehalose in their backbones yield high cellular delivery efficiency of plasmid DNA (pDNA).<sup>19</sup> Tseng et al. have shown that the presence of free trehalose in cell culture media enhances plasmid DNA (pDNA) delivery by polyethylenimine (PEI)-based complexes to various cell lines.<sup>20</sup> Polymers of trehalose have been found to induce autophagy in the brain; its presence has been linked to neuroprotective effects in cases of Huntington, Parkinson, and prion diseases.<sup>21,22</sup> Wada et al. have demonstrated that a statistical copolymer of trehalose and acrylamide inhibits the aggregation of amyloid  $\beta$  peptide, associated with Alzheimer's disease.<sup>23</sup> More recently, Mancini et al. reported that lysozyme covalently attached to *p*-formylpolystyrene modified with trehalose via an acetonide moiety is capable of imparting both lyo- and heat protectant properties to this enzyme.<sup>24</sup>

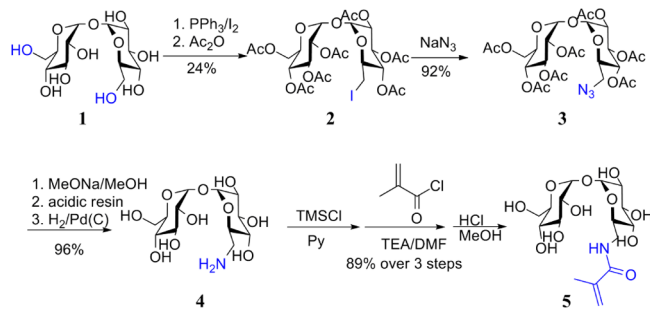
Herein, we report the synthesis of a methacrylamido trehalose monomer, its subsequent polymerization to poly(methacrylamidotrehalose) or “poly(trehalose)”, followed by chain extension with aminoethylmethacrylamide (AEMA). We also demonstrate the exceptional properties of these new polymers that are used to complex siRNA (into interpolyelectrolyte complexes or polyplexes) and promote high cellular delivery of siRNA (Figure 1). Block copolyacrylates containing this poly(trehalose) motif are found to stably complex siRNA exposing a coating of poly(trehalose) on the nanocomplex surface. We hypothesized that the polymeric nature would impart an increase in the local viscosity on the particle surface, thus enhancing vitrification of the surface-bound water and colloidal stability during lyophilization and resuspension.<sup>25</sup> For the first time, we demonstrate that this poly(trehalose) motif

enhances colloidal stability of siRNA nanocomplexes in salt, serum, and during the lyophilization process. We show that an aqueous solution containing polyplexes is able to be frozen, lyophilized to dryness (causing physical aggregation), and then resuspended back into polyplexes with the same size profile, while control systems lacking poly(trehalose) rapidly aggregated in these conditions. In addition, we have found that poly(trehalose) polyplexes containing siRNA afford high delivery efficiency and gene knockdown in glioblastoma cells, which are known to overexpress glucose transporter-1.<sup>26</sup> We also reveal that biological efficacy (gene knockdown) does not change after lyophilization and aqueous resuspension. We believe that block copolyacrylates containing this poly(trehalose) motif offer a unique combination of both stabilizing and targeting potential, which offers an effective and creative platform to be further developed as a nanoparticle surface coating for various delivery applications.

## RESULTS AND DISCUSSION

**Synthesis of Monomer and Polymers.** Our development of a synthetic scheme to yield a functionalized, trehalose-containing monomer was guided by two criteria: (i) the linker length connecting trehalose and a polymerizable functionality should be small, and (ii) the synthesis should reduce/avoid the use of lengthy and scale-limiting purification procedures. However, the  $C_2$  symmetry of trehalose (**1**, Scheme 1) poses an inherent challenge in yielding the desired asymmetrically functionalized monomer.<sup>27</sup> Due to practical considerations for our study, an approach was taken to monofunctionalize trehalose modeled from the procedure of Wada et al. with

**Scheme 1.** Synthesis of 6-Methacrylamido-6-deoxytrehalose (MAT)



important improvements (Scheme 1).<sup>23</sup> Triphenylphosphine-iodine was used to produce a mixture of three species, diiodo-, monoiodo-, and unmodified trehalose. This mixture was acetylated and the desired per-acetylated monoiodo-trehalose **2** was obtained after column chromatography in 24% yield. The substitution of the iodide for azide yielded **3** (92%), which was further deprotected and reduced by hydrogenation, affording 6-amino-6-deoxytrehalose (**4**, 96%). The hydroxyl groups in compound **4** were protected with TMS and the amine was reacted with methacryloyl chloride. After the aqueous workup the TMS-ylated methacrylamide derivative was extracted with hexanes and subsequently deprotected with HCl in methanol to yield the monomer **5** in 93% yield (see Supporting Information [SI] for details).

To prepare poly(trehalose), we employed reversible addition–fragmentation chain transfer (RAFT) polymerization because this mechanism offers polymers with low dispersity, provides control over molecular weight, tolerates the presence of many reactive functional groups, and allows for synthesis of multiblock architectures.<sup>28–30</sup> Polymer syntheses were conducted using 4-cyano-4-(propylthiocarbonothioylthio)-pentanoic acid (CPP) or propylthiocarbonothioylthio-terminated polytrehalose as the chain transfer agent and 4,4'-azobis(4-cyanovaleric acid) (V-501) as the initiator (Figure 2a).

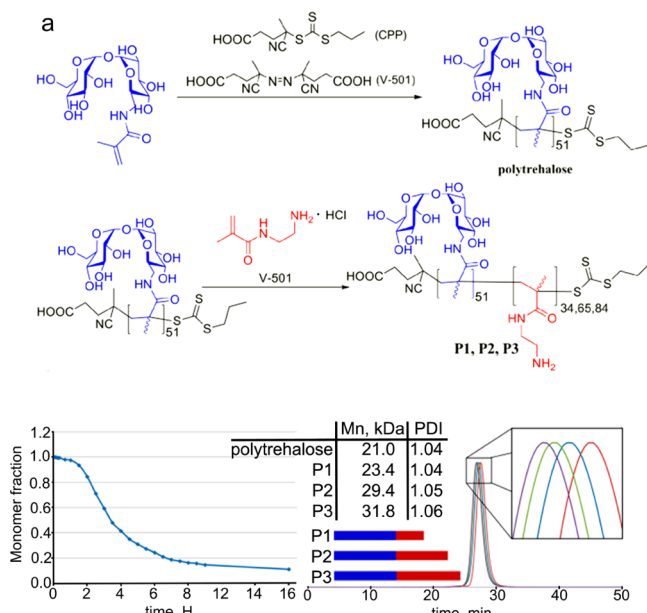


**Figure 2.** Polymer synthesis and characterization. (a) Synthesis of polytrehalose and diblock polymers **P1**, **P2**, **P3**. (b) Monomer consumption based on integration of the vinyl proton in <sup>1</sup>H NMR experiments in the RAFT polymerization of **5**. (c) SEC traces of polytrehalose (red), **P1** (blue), **P2** (green), and **P3** (purple). Schematic blocks represent the relative trehalose- and amine-containing blocks in polymers **P1**, **P2**, and **P3**.

Kinetics were established in a water–methanol mixture buffered with AcOH/AcONa and used to create poly(trehalose) **6** with a degree of polymerization of 51 (Figure 2b). This glycopolymer was then used as macro chain transfer agent (macroCTA) and chain extended with aminoethylmethacrylamide (AEMA) hydrochloride to create three diblock polymers **P1**, **P2**, and **P3**, that have 34, 65, and 84 AEMA repeat units respectively. For comparison, two control polymers were also created to assess the role of poly(trehalose) block

copolycations in stabilization of siRNA polyplexes to a polycation containing a known stabilizing agent, PEG-P(AEMA), and a motif lacking a stabilizing polymer, P(AEMA) (SI). All polymers were analyzed by size exclusion chromatography equipped with multiangle light-scattering detector to reveal narrow peaks and expected shifts in elution times with increases in polymer molecular weight (Figure 2c). Polymerizations were well-controlled, providing the final polymers with low dispersity (polydispersity indeces were <1.06 for the poly(trehalose) systems, see SI for details).

**Physical Properties of Poly(trehalose) Polymers.** The aforementioned lyoprotective properties of trehalose have been largely attributed to its ability to decrease water crystallization around biological membranes and proteins and to decrease the energy associated with phase transitions of H<sub>2</sub>O (crystallization and melting).<sup>31</sup> To examine whether poly(trehalose) retained this property, we analyzed both trehalose and poly(trehalose) solutions of various concentrations via differential scanning calorimetry (DSC). Poly(trehalose) exhibited similar properties to trehalose in depressing both the heat of ice melting ( $H_m$ ) and the heat of water crystallization ( $H_{cr}$ ), up to a concentration of 2.2 mol %, and was even more effective than trehalose itself at higher solution concentrations (Figures 2b and 3a). At 5 mol %, poly(trehalose) lowers  $H_m$  by an additional 24 J/g and  $H_{cr}$  by an additional 35 J/g compared to trehalose; that concentration corresponds to about 23 water molecules per trehalose residue, which is nearly twice as many water molecules as are present in the hydration sphere of trehalose alone.<sup>32</sup>

It is known that high viscosity favors glass formation over crystallization and the observed enhanced efficiency is likely a result of the increased viscosity of the poly(trehalose) solution compared to that of a solution of trehalose.<sup>33,34</sup> Importantly, it was also discovered that the poly(trehalose) solution can be cooled below 0 °C without noticing the onset of crystallization (Figure 3c). These data pointed towards the promising attributes of utilizing a poly(trehalose) motif as a barrier to increase payload stability and decrease nanocomplex aggregation.

To examine the surface properties that this poly(trehalose) motif imparts to nanocomplexes with polynucleotides, several polyplex formulations between siRNA and each diblock copolymer **P1**–**P3** were prepared and examined for binding and polyplex formation via transmission electron microscopy (Figure S2 in SI), gel electrophoresis (Figure S3 in SI), and dynamic light scattering (Figure 3d and 3e). In addition, these techniques were used to assess aggregation. As evident from gel shift assay data (Figure S3 in SI), **P1**, **P2**, and **P3** readily bind siRNA at low N/P ratios (molar formulation ratio between the number of amines on the diblock copolymer and the phosphate groups on siRNA) of 3, 3, and 2, respectively. These polyplex formulations also demonstrated high stability from aggregation in culture media (both in the absence and presence of serum) containing physiological salt concentrations. Polyplex hydrodynamic diameters were observed between 150 to 200 nm in OptiMEM and somewhat larger in serum-containing DMEM (Figures 3d, 3e). The slight increase in size in the presence of serum is suggestive of interactions between polyplexes and serum components, likely proteins. These interactions could result from physical entanglement (entrapment) of proteins<sup>35</sup> or via hydrogen bonding.<sup>36</sup> However, this interaction is likely weak<sup>23</sup> and, as can be seen from Figure 3d, does not compromise the stability of nanoparticles. The polyplexes

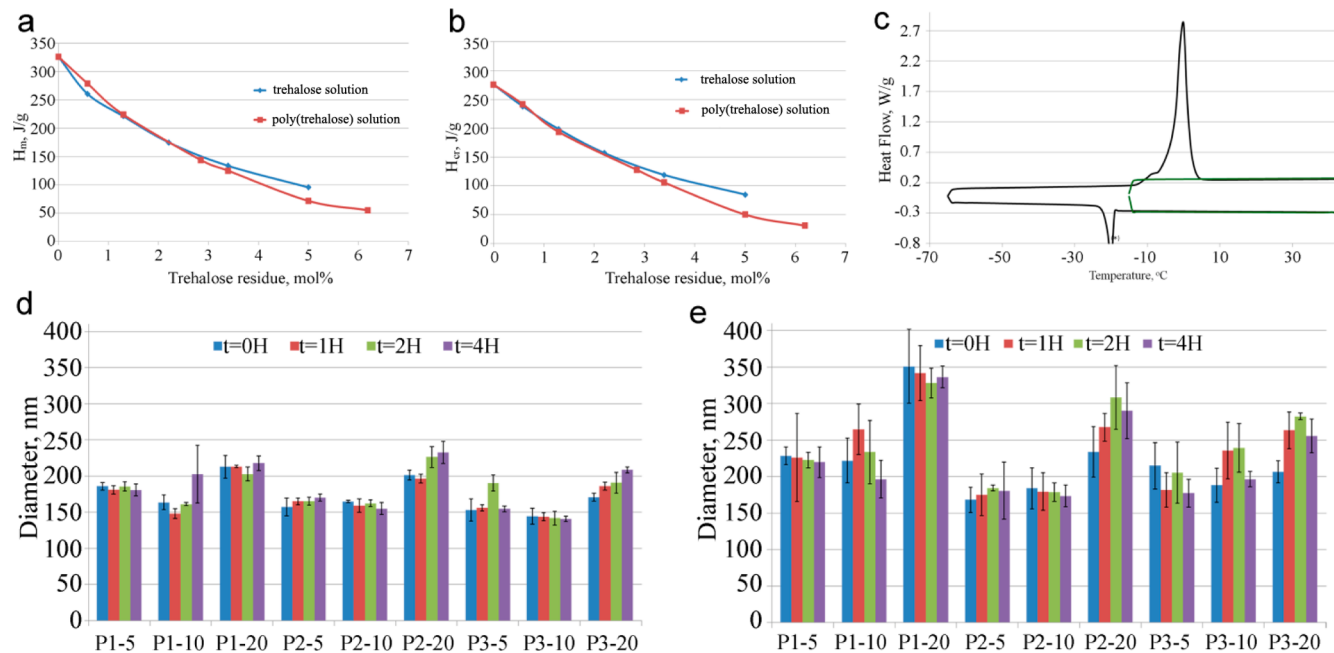


**Figure 3.** Physical properties of polytrehalose and polyplexes formulated with the polytrehalose block copolymers. (a) Depression in heats of ice melting,  $H_m$ , and (b) water crystallization,  $H_w$ , of trehalose and polytrehalose solutions at various concentrations. Data was not obtained for trehalose solutions above 5 mol % due to solubility limitations. (c) Differential scanning calorimetry (DSC) of a 2.2 mol % solution of polytrehalose. Isothermal conditioning was applied for both cool-heat cycles at the lowest temperature for 30 min. The graphical representation of the exothermic peak does not display a ‘loop’ (\*) which results from overcooling. The hydrodynamic diameters determined via dynamic light scattering (DLS) of polyplexes formed between siRNA and diblock polymers **P1**, **P2**, and **P3** at N/P ratios of 5 and 10 in OptiMEM (d), and DMEM containing 10% FBS (e) (mean  $\pm$  s.d.,  $n = 3$ ). In (d) and (e), labels P- $n$  signify polymer-N/P ratio.

formulated with the control polycations, PEG-P(AEMA) and P(AEMA) revealed substantial aggregation in these media (Figures S5c, S5b in SI).

The ability of a nanocarrier system to stabilize various cargo from degradation and aggregation during storage is an important feature in designing nucleic acid carriers for clinical use. For example, Kasper et al. have shown that PEGylated poly(ethyleneamine) polyplexes containing plasmid DNA can be stabilized from lyophilization and resuspension by creating formulations with excipients such as free trehalose.<sup>37</sup> To demonstrate the cryo- and lyo-protective properties that poly(trehalose) imparts on the polyplexes, lyophilization was performed followed by resuspension of the polyplex formulas in aqueous conditions. It should be noted that no excipients, nor separate cryo- or lyo-protectants were added to the formulation. After freezing, the polyplex solutions were completely lyophilized to isolate the polyplexes as a white solid (this process also physically aggregates the polyplexes). Interestingly, at both N/P ratios examined (5 and 10), subsequent resuspension of the solid polyplex powder in water yielded isolated nanoparticles that retained their compact size and shape, as determined via DLS (Figure S4 in SI) and transmission electron microscopy (TEM) imaging (Figure 4), while polyplexes formed with the control polymers, PEG-P(AEMA) and P(AEMA), revealed substantial aggregation after lyophilization (Figure S5c in SI). Importantly, the polyplexes stabilize siRNA from degradation during lyophilization and reconstitution as biological activity toward siRNA-mediated gene down-regulation is fully retained (vide infra, Figure 7d). At both N/P ratios, polymer **P1**, that has the greatest trehalose content among the three synthesized polymers, appeared to yield optimal results for facilitating the stable resuspension of the polytrehalose-coated polyplexes (Figure 4 and Figure S4 in

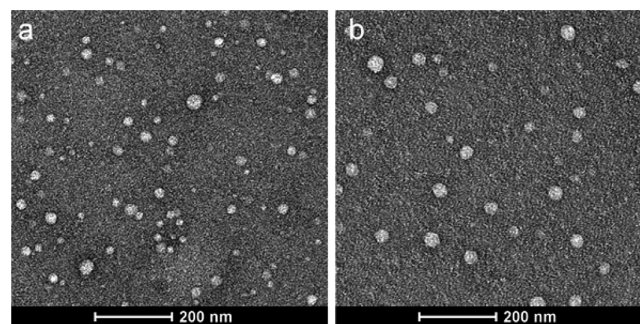


**Figure 4.** TEM of polyplexes formulated with **P1** and siRNA at an N/P ratio of 10. (a) Image of **P1** polyplexes freshly prepared in water (average core diameter:  $22 \pm 4$  nm) and (b) image of **P1** polyplexes that have been lyophilized to a solid powder and resuspended in water (average core diameter:  $31 \pm 7$  nm).

SI). TEM imaging, used to visually evaluate the effect of lyophilization on the size and shape of the poly(trehalose) containing polyplexes made from **P1**, revealed visual images of the polyplexes supporting the DLS data above (Figure 3). Following lyophilization and reconstitution, these polyplexes did not change in size and shape (Figures 4a and 4b, respectively), supporting the DLS data in Figure S4 in SI. It has been reported that polyplexes composed of block copolymers can form “core–shell” structures in solution.<sup>38,39</sup> The difference in size measured in the TEM images as compared to that observed via DLS could be due changes in the corona structure caused by dehydration in TEM sample preparation (DLS measures hydrodynamic radius).<sup>40</sup> Additionally, the negative stain, uranyl acetate, is known to bind to phosphate moieties on nucleic acids, which may allow

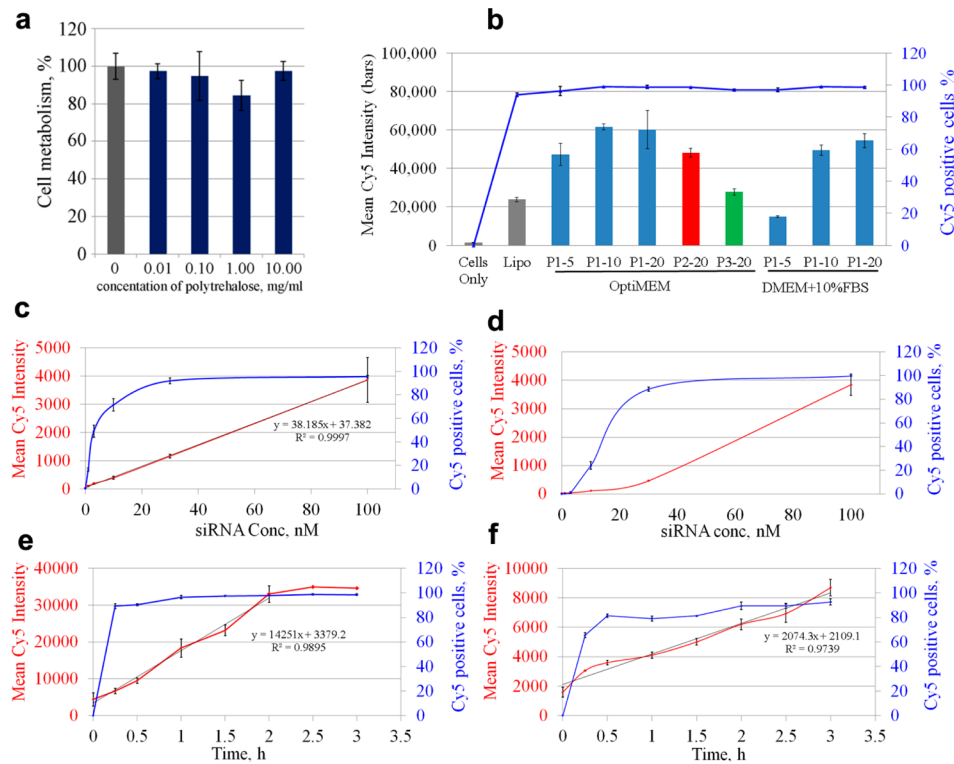


**Figure 5.** (a) Cell viability assessed by MTT assay after the incubation with various concentrations of polytrehalose (mean  $\pm$  s.d.,  $n = 3$ ). (b) Cellular uptake by U-87 cells at siRNA concentration of 100 nM (mean  $\pm$  s.d.,  $n = 3$ ). (c) Dependence of cellular uptake by U-87 cells on siRNA concentration using polymer P1 at N/P of 10 in (c) OptiMEM (mean  $\pm$  s.d.,  $n = 3$ ) or (d) DMEM with 10% FBS (mean  $\pm$  s.d.,  $n = 3$ ). (e) The rate of the uptake of P1–P10 polyplexes at 100 nm siRNA concentration in (e) OptiMEM (mean  $\pm$  s.d.,  $n = 3$ ) or (f) DMEM with 10% FBS (mean  $\pm$  s.d.,  $n = 3$ ). Red lines indicate Mean Cy5 intensity data; blue lines denote Cy5-positive cells (%).

visualization of the core only, resulting in observing a smaller polyplex size via TEM.<sup>41</sup>

**Cytotoxicity.** For siRNA down-regulation to be effective, it is very important for the polyplexes to exhibit little to no cytotoxicity. Poly(trehalose) was found to be nontoxic with U-87 cells up to a concentration of 10 mg/mL (Figure 5a). Moreover, siRNA polyplexes formulated with P1, P2, and P3 polymers show no significant cytotoxicity at all N/P ratios tested (Figure S6 in SI) whereas the control polymers PEG-P(AEMA) and P(AEMA) exhibited toxicity (Figure S21 in SI). The low toxicity granted further biological evaluation of these polymers.

**Cellular Uptake.** Upon administration and biodistribution, cellular internalization is the first barrier that polyplexes encounter during the delivery process. To a large degree, this is defined by the interactions between the nanoparticle surface and cell membranes. We have reported previously, that incorporation of another glycopolymer with a poly(glucose) motif into nanoparticle formulations improves cellular uptake by glioblastoma cells.<sup>42</sup> It is also known that glioblastoma cells not only overexpress GLUT-1<sup>26</sup> but also that this glucose transporter can be employed by viruses (biological nanoparticles) for cellular entry.<sup>43</sup> Therefore, the ability of poly(trehalose)-coated polyplexes to undergo cellular internalization in glioblastoma cells was studied in detail.

Polyplexes were formulated with fluorescently labeled siRNA, and the extent of their internalization by U-87 glioblastoma cells was measured with flow cytometry. All three polymers yielded efficient delivery of siRNA to cells and did so homogeneously across the cell population. More than 90% of the cells tested positive for siRNA with all formulations studied

(Figure 5b). polymer P1 was the most efficient among the three polymers tested, delivering the greatest number of siRNA copies per cell (as indicated by the greatest mean cellular fluorescence). It is important to note that polyplexes formed with each of the three polymers at N/P of 20 have similar sizes and  $\zeta$ -potentials (Figure S4 in SI). However, the primary difference between the formulations is the poly(trehalose) content. Polymer P1 contains 83% of poly(trehalose) by mass, whereas P2 and P3 contain 71% and 66%, respectively, which suggests that poly(trehalose) could have a positive impact on the efficiency of U-87 uptake of these nanoparticles. On the basis of these initial uptake results, polymer P1 at N/P ratio 10 was chosen for further investigations.

The influence of siRNA concentration (dose) in the transfections media on cellular uptake was assessed (Figures 5c and 5d). It was observed that the number of siRNA molecules that are internalized by cells is linearly proportional to the concentration of siRNA in serum containing DMEM (Figure 5d), and with nearly perfect linearity ( $R^2 > 0.99$ ) in serum-free OptiMEM (Figure 5c). The deviation from the linear dependence in serum containing DMEM is likely due to uptake in the presence of serum having slower kinetics. This finding shows that the amount of siRNA delivered to the cells can be controlled by altering the siRNA concentration in the media. Importantly, delivery is not saturated even at 100 nM siRNA concentration, meaning that higher doses of siRNA containing polyplexes could be used, if necessary.

The rate of the uptake was studied at 100 nM siRNA concentration and revealed interesting phenomena (Figures 5e and 5f). First, it is clear that poly(trehalose)-coated nanoparticles internalize homogeneously across the cell population:

more than 80% of U-87 cells are transfected with siRNA within the first 30 min. More importantly, the amount of siRNA delivered is linearly dependent on time in both serum-free and serum-containing media, with  $R^2$  values of 0.99 and 0.97, respectively. Thus, the rate of internalization is constant with time (zeroth order). In addition, in serum-free media, the fluorescence reaches a plateau after 2 h, the cell has reached an uptake equilibrium early in the transfection process. At this point, we are speculating specific receptor involvement in the uptake of the poly(trehalose)-coated polyplexes. It is worth noting that GLUT-1 operates in a saturated mode at physiological conditions,<sup>44</sup> it is overexpressed in glioblastoma cells,<sup>26</sup> and as mentioned is used by viruses for cellular entry.<sup>43</sup> Considering the obtained uptake results and the known correlation between GLUT-1 and poor response to treatment in several types of cancer<sup>45–47</sup> further investigation into poly(trehalose)-promoted cellular entry is warranted.

Efficient uptake was also observed with confocal microscopy using Cy5-labeled siRNA and FITC-labeled polymer **P1** (Figure 6). After the first hour of incubation, the punctate

express luciferase. The extent of gene down-regulation was assessed by the decrease in light production via luciferase assay. All three polymers promoted significant gene knockdown in OptiMEM (Figure 7a). The efficiency of gene down-regulation increased with an increase in N/P ratio and, at an N/P of 20, was at 80% gene knockdown (similar to lipofectamine). In serum-containing DMEM only polymer **P1** was capable of promoting gene knockdown. The variation in gene silencing efficiency in OptiMEM vs DMEM containing 10% serum (Figures 7a and 7b) is likely due to biotransformation. It has been reported that, in serum, proteins may bind to the polyplex and form a layer on the surface, thus inhibiting polyplex binding to the cell membrane and/or destabilizing polyplexes via competitive interactions.<sup>48</sup> We also investigated the dose response of the gene down-regulation. In contrast to the uptake response, which was linearly dependent on siRNA concentration (Figures 5c and 5d), the dependence of the extent of gene knockdown exhibited a logarithmic dependence on siRNA concentration (Figure 7c). The IC<sub>50</sub> value for luciferase gene down-regulation promoted by **P1** at N/P 10 with siRNA was calculated to be 19 nM. With the control polyplexes formulated with PEG-P(AEMA) and P(AEMA), gene knockdown was found, which increased with N/P ratio. However, a significant off-target effect was noticed where polyplexes formulated with siCON also showed significant gene knockdown, signifying toxicity of the control formulations.

It was of interest to probe the ability of the poly(trehalose)-containing nanoparticles to retain siRNA-mediated gene down-regulation after lyophilization and subsequent resuspension. As previously mentioned, polymer **P1** was chosen for these studies because it contains the largest amount of poly(trehalose) among three polymers and it was found to promote the optimal polyplex resuspension after lyophilization. Also, it was revealed to be the most effective vehicle for siRNA delivery. Therefore, we hypothesized that it would impart the greatest ability to preserve the biological activity of polyplexes.

Formulations of **P1**-siRNA polyplexes were lyophilized, and the dry powder was resuspended in RNase-free water and then with cell culture media. Gene down-regulation by the resuspended polyplexes was compared to freshly prepared polyplexes made with the same polymer (Figure 7d). The extent of luciferase gene down-regulation induced by the lyophilized/resuspended polyplexes was identical to that observed with the freshly prepared analogs whereas activity was lost for the control, lipofectamine (Figure 7d), after lyophilization.

This result shows that this poly(trehalose) motif displayed on the surface of the polyplexes, promotes protection of sensitive macromolecules during the freeze-drying process. Using confocal microscopy, we have investigated fluorescently labeled polyplexes after uptake into U-87 cells for 48 h, when gene down-regulation was measured (Figure S7 in SI). Despite the active trafficking observed immediately following the uptake as discussed above, the punctate nature of the fluorescence remains visually unchanged up to 12 h (Figure S7 in SI). At 24 h, however, there is a sharp drop in Cy5 fluorescence, indicating that siRNA release takes place between 12 and 24 h post transfection. At the same time FITC fluorescence that corresponds to the polymer FITC-P1 is maintained throughout the microscopy experiment (up to 48 h, Figure S7 in SI) and remains punctate.

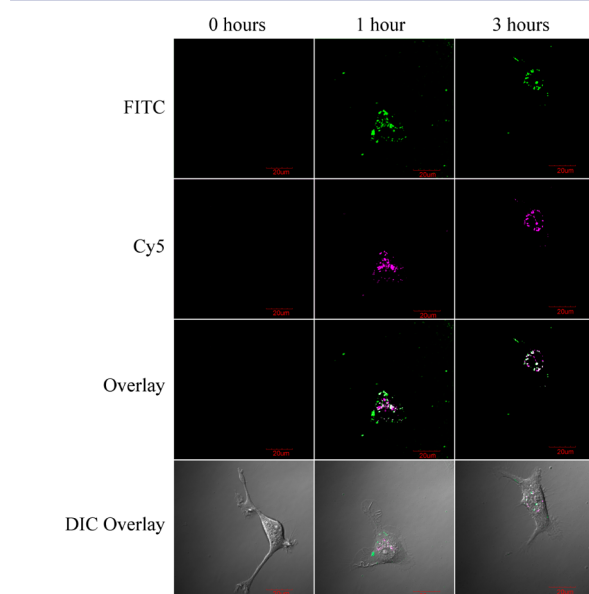


**Figure 6.** Confocal microscopy of U-87 cells transfected with Cy5-labeled siRNA (magenta) and FITC-labeled **P1** (green) at N/P ratio 10. Cells were imaged at 0, 1, and 3 h after transfection (the time point of 0 = cells only).

nature of the fluorescence was observed in both Cy5 and FITC distributed throughout the cytoplasm. Distribution of the polyplexes inside the whole cell, rather than near the cellular membrane, indicates that trafficking of the particles is a rapid process. To visualize this polyplex trafficking, live cell imaging was used to compile a time-lapse video of **P1** polyplexes (formulated at N/P 10) trafficking in U-87 cells for 6 min, at a time point of 2 h after transfection (see SI video). The video reveals that the polymer and siRNA are associated as discrete polyplexes and active trafficking appears to take place as the polyplexes are shuttled around the cytoplasm.

**Gene Down-Regulation.** The major goal of the biological investigation was to establish the cellular internalization properties of the poly(trehalose)-containing nanoparticles and the ability of these systems to down-regulate a target gene. The evaluation was performed in U-87 glioblastoma cells that stably

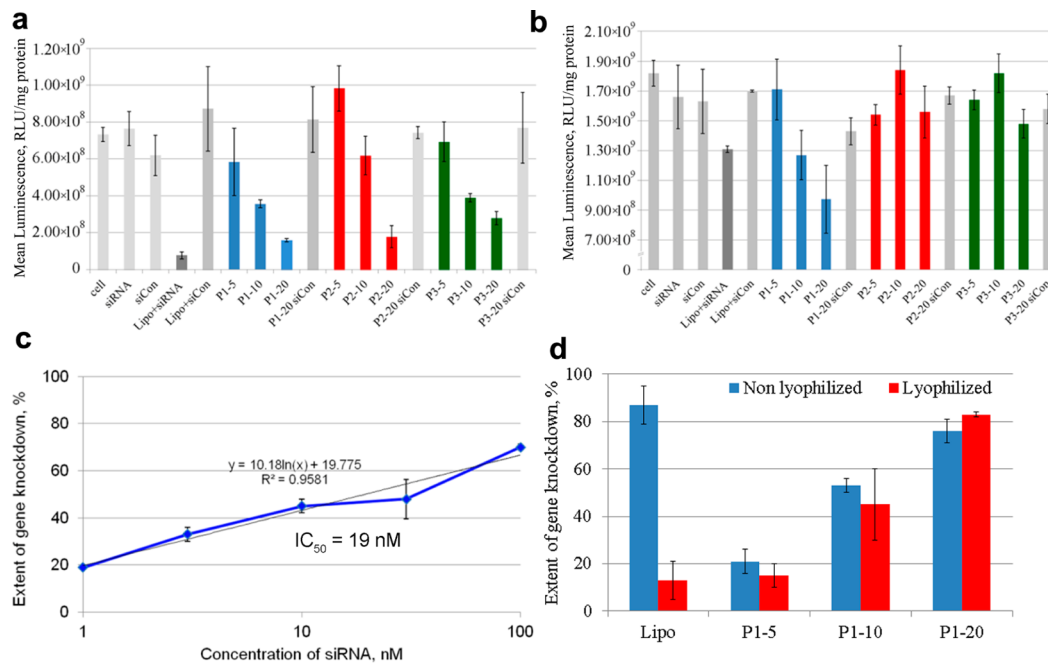


**Figure 7.** Luciferase gene knockdown in luciferase-expressing U-87 cells. Cells were transfected in (a) serum-free OptiMEM or (b) DMEM containing 10% serum (mean  $\pm$  s.d.,  $n = 3100$  nM siRNA). (c) Evaluation of the efficiency of gene down-regulation on siRNA concentration. Transfections were performed in OptiMEM (mean  $\pm$  s.d.,  $n = 3$ ). (d) Comparison of target gene down-regulation in luciferase-expressing U-87 cells between freshly prepared P1 polyplexes and previously lyophilized P1 polyplexes. Transfections were performed at an siRNA concentration of 100 nM in OptiMEM (mean  $\pm$  s.d.,  $n = 3$ ). Labels signify “polymer name-N/P ratio”, “Lipo” = lipofectamine, “siCon” = siRNA with scrambled sequence (negative control), “siRNA” = siRNA only (no delivery vehicle), “cells” = cells-only negative control (no siRNA or delivery vehicle treatment).

## CONCLUSION

The field of siRNA-based therapeutics has great potential, yet advanced materials-based delivery systems still need to be engineered. The poly(trehalose) motif presented in this report has many valuable and interesting properties making it a candidate for inclusion within the outer layer of macromolecules and nanosystems. Poly(trehalose) and diblock polymers containing this motif can be readily synthesized with a predefined length and low dispersity via RAFT polymerization without use of protecting groups. It was demonstrated that poly(trehalose) lowers the energy of phase transition (liquid to solid, and solid to liquid) of an aqueous solution and this property allowed us to lyophilize siRNA polyplexes and resuspend them freely in a solution without loss of biological function.

Poly(trehalose) was shown to promote polyplex internalization by U-87 glioblastoma cells and did not exhibit cytotoxicity at all concentrations tested (up to 10 mg/mL). The cellular uptake had zeroth-order kinetics in both tested cell culture media and is directly proportional to the concentration of poly(trehalose)-containing polyplexes in the media. On the basis of the results of the uptake experiments we speculate that a carbohydrate-binding receptor could be responsible for the high efficiency of uptake.

The successful use of poly(trehalose) block copolymerizations for siRNA delivery was demonstrated in luciferase expressing U-87 glioblastoma cells. This activity was preserved following the lyophilization of polyplexes, potentially enabling the storage of the therapeutic siRNA formulations as dry powders and simplifying transportation. Indeed, the remarkable properties demonstrated by poly(trehalose) make it particularly interesting stabilizing structure for study in macromolecule and

nanoparticle formulations including micelles, liposomes, proteins, and various metal-based nanoparticle systems.

## ASSOCIATED CONTENT

### Supporting Information

Materials, synthetic procedures, characterization, details of investigation of materials properties and procedures, and cell culture experiments and procedures, confocal microscopy. This material is available free of charge via the Internet at <http://pubs.acs.org>.

## AUTHOR INFORMATION

### Corresponding Author

treineke@umn.edu

### Present Address

<sup>§</sup>Baylor College of Medicine, Department of Pharmacology, Houston, TX 77030.

### Notes

The authors declare no competing financial interest.

## ACKNOWLEDGMENTS

We acknowledge funding of this project by the NIH Director’s New Innovator Program (DP2OD006669-01) and the Camille and Henry Dreyfus Foundation.

## REFERENCES

- (1) Knop, K.; Hoogenboom, R.; Fischer, D.; Schubert, U. S. *Angew. Chem., Int. Ed.* **2010**, *49*, 6288–6308.
- (2) Chanan-Khan, A.; Szebeni, J.; Savay, S.; Liebes, L.; Rafique, N. M.; Alving, C. R.; Muggia, F. M. *Ann. Oncol.* **2003**, *14*, 1430–1437.
- (3) Szebeni, J. *Toxicology* **2005**, *216*, 106–121.
- (4) Dewachter, P.; Mouton-Faivre, C. *Allergy* **2005**, *60*, 705–706.

- (5) Ishida, T.; Harada, M.; Wang, X. Y.; Ichihara, M.; Irimura, K.; Kiwada, H. *J. Controlled Release* **2005**, *105*, 305–317.
- (6) Ishida, T.; Kashima, S.; Kiwada, H. *J. Controlled Release* **2008**, *126*, 162–165.
- (7) Ishida, T.; Kiwada, H. *Int. J. Pharm.* **2008**, *354*, 56–62.
- (8) Herold, D. A.; Keil, K.; Bruns, D. E. *Biochem. Pharmacol.* **1989**, *38*, 73–76.
- (9) Hinds, K. D. *Biomaterials for Delivery and Targeting of Proteins and Nucleic Acids*; CRC: Boca Raton, FL, 2005.
- (10) Han, S.; Kim, C.; Kwon, D. *Polymer* **1997**, *38*, 317–323.
- (11) Teramoto, N.; Sachinvala, N.; Shibata, M. *Molecules* **2008**, *13*, 1773–1816.
- (12) Benaroudj, N.; Lee, D. H.; Goldberg, A. L. *J. Biol. Chem.* **2001**, *276*, 24261–24267.
- (13) Hagen, S. J.; Hofrichter, J.; Eaton, W. A. *Science* **1995**, *269*, 959–962.
- (14) Clegg, J. S.; Seitz, P.; Seitz, W.; Hazlewood, C. F. *Cryobiology* **1982**, *19*, 306–316.
- (15) Ramlov, H.; Westh, P. *Cryobiology* **1992**, *29*, 125–130.
- (16) Sømme, L. *Eur. J. Entomol.* **1996**, *93*, 349–358.
- (17) Adams, R. P.; Kendall, E.; Kartha, K. *Biochem. Syst. Ecol.* **1990**, *18*, 107–110.
- (18) Crowe, J. H.; Crowe, L. M.; Oliver, A. E.; Tsvetkova, N.; Wolkers, W.; Tablin, F. *Cryobiology* **2001**, *43*, 89–105.
- (19) Srinivasachari, S.; Liu, Y.; Zhang, G.; Prevette, L.; Reineke, T. *M. J. Am. Chem. Soc.* **2006**, *128*, 8176–8184.
- (20) Tseng, W. C.; Tang, C. H.; Fang, T. Y.; Su, L. Y. *Biotechnol. Prog.* **2007**, *23*, 1297–1304.
- (21) Sarkar, S.; Davies, J. E.; Huang, Z.; Tunnacliffe, A.; Rubinsztein, D. C. *J. Biol. Chem.* **2007**, *282*, 5641–5652.
- (22) Casarejos, M.; Solano, R.; Gómez, A.; Perucho, J.; de Yébenes, J.; Mena, M. *Neurochem. Int.* **2011**, *58*, 512–520.
- (23) Wada, M.; Miyazawa, Y.; Miura, Y. *Polym. Chem.* **2011**, *2*, 1822–1829.
- (24) Mancini, R. J.; Lee, J.; Maynard, H. D. *J. Am. Chem. Soc.* **2012**, *134*, 8474–8479.
- (25) Crowe, J. H.; Carpenter, J. F.; Crowe, L. M. *Annu. Rev. Physiol.* **1998**, *60*, 73–103.
- (26) Jensen, R. L.; Chkhcheidze, R. Part 1 of *Gliomas: Glioblastoma*. In *Tumors of the Central Nervous System*; Hyat, M. A., Ed.; Springer: New York, 2011; Vol. 1, p 99–108.
- (27) Patel, M. K.; Davis, B. G. *Org. Biomol. Chem.* **2010**, *8*, 4232–4235.
- (28) Moad, G.; Rizzardo, E.; Thang, S. H. *Aust. J. Chem.* **2005**, *58*, 379–410.
- (29) Moad, G.; Rizzardo, E.; Thang, S. H. *Aust. J. Chem.* **2006**, *59*, 669–692.
- (30) Moad, G.; Rizzardo, E.; Thang, S. H. *Aust. J. Chem.* **2009**, *62*, 1402–1472.
- (31) MacLaughlin, F. C.; Mumper, R. J.; Wang, J.; Tagliaferri, J. M.; Gill, I.; Hinchcliffe, M.; Rolland, A. P. *J. Controlled Release* **1998**, *56*, 259–272.
- (32) Branca, C.; Magazù, S.; Maisano, G.; Migliardo, F.; Migliardo, P.; Romeo, G. *J. Phys. Chem. B* **2001**, *105*, 10140–10145.
- (33) Freed, K. F.; Edwards, S. *J. Chem. Phys.* **1974**, *61*, 3626–3633.
- (34) Uhlmann, D. *J. Non-Cryst. Solids* **1972**, *7*, 337–348.
- (35) Hong, W.; Bielinska, A. U.; Mecke, A.; Keszler, B.; Beals, J. L.; Shi, X.; Balogh, L.; Orr, B. G.; Baker, J. R., Jr.; Banaszak Holl, M. M. *Bioconjugate Chem.* **2004**, *15*, 774–782.
- (36) Villarreal, M. A.; Díaz, S. B.; Disalvo, E. A.; Montich, G. G. *Langmuir* **2004**, *20*, 7844–7851.
- (37) Kasper, J. C.; Schaffert, D.; Ogris, M.; Wagner, E.; Friess, W. J. *Controlled Release* **2011**, *151*, 246–255.
- (38) Ziebarth, J.; Wang, Y. *J. Phys. Chem. B* **2010**, *114*, 6225–6232.
- (39) Nakai, K.; Nishiuchi, M.; Inoue, M.; Ishihara, K.; Sanada, Y.; Sakurai, K.; Yusa, S.-i. *Langmuir* **2013**, *29*, 9651–9661.
- (40) Li, X.; Mya, K. Y.; Ni, X.; He, C.; Leong, K. W.; Li, J. *J. Phys. Chem. B* **2006**, *110*, 5920–5926.
- (41) Nielsen, P. E. In *DNA-Protein Interactions, Principles and Protocols*; 3rd ed.; Moss, T., Leblanc, B., Eds.; Springer: New York, 2009; Vol. 543, pp 87–96.
- (42) Buckwalter, D. J.; Sizovs, A.; Ingle, N. P.; Reineke, T. M. *ACS Macro Lett.* **2012**, *1*, 609–613.
- (43) Manel, N.; Kim, F. J.; Kinet, S.; Taylor, N.; Sitbon, M.; Battini, J. L. *Cell* **2003**, *115*, 449–459.
- (44) Elsas, L. J.; Longo, N. *Annu. Rev. Med.* **1992**, *43*, 377–393.
- (45) Airley, R.; Lancaster, J.; Davidson, S.; Bromley, M.; Roberts, S.; Patterson, A.; Hunter, R.; Stratford, I.; West, C. *Clin. Cancer Res.* **2001**, *7*, 928–934.
- (46) Airley, R. E.; Lancaster, J.; Raleigh, J. A.; Harris, A. L.; Davidson, S. E.; Hunter, R. D.; West, C. M. L.; Stratford, I. *J. Int. J. Cancer* **2003**, *104*, 85–91.
- (47) Jensen, R. L. *J. Neurooncol.* **2009**, *92*, 317–335.
- (48) Karmali, P. P.; Simberg, D. *Expert Opin. Drug Delivery* **2011**, *8*, 343.